

Melting Effect of Hole-Injecting Layer on the Performance of Passive Matrix Organic Light-Emitting Displays

Youngkyoo Kim*, Dongkwon Choi and Hwajeong Kim

Organic Nanoelectronics Laboratory, Department of Chemical Engineering, Kyungpook National University, Daegu 702-701, Republic of Korea

Abstract: Here we report improved operation stability of passive matrix organic light-emitting displays (PM-OLED) by melting a hole-injecting layer (HIL) that is the first organic layer contacting anode. The PM-OLED displays fabricated in this work are consisted of 128×128 pixels in which each pixel has a dimension of 200μm×200μm. The exact thermal transition behaviour of hole-injecting material was first examined using a differential scanning calorimeter in order to decide the melting temperature for the HIL melting process (300°C/3min). Results show that the display with the untreated (as-coated) HIL exhibited large leakage current which eventually resulted in damages (black cross-talk lines) to the display during operation. However, no cross-talk defect was observed for the PM-OLED display with the thermally treated (melted) HIL, which was supported by the absence of leakage current at reverse bias.

Since the breakthrough works on organic light-emitting devices (OLED) based on either low-molecular-weight materials (i.e., small molecules) [1] or polymers [2], OLED displays are now in market even though their applications are limited to small size display for MP3 players, mobile phones, car front panel devices, shavers, etc [3, 4]. This successful debut of OLED display into market can be mainly attributed to remarkable advances in organic semiconductor materials and process technology [3-5].

However, these OLED displays do still suffer from their short lifetime though the thermal stability of organic materials themselves has been significantly improved when it comes to the test device measurement [4, 6, 7]. In case of OLED displays made using small molecules, it has been reported that a progressive electrical short (PES) phenomenon is responsible for the degradation of display pixels during long time operation [8]. This report claimed that the PES phenomenon is closely related to the formation of unstable defects in organic layers which eventually leads to catastrophic degradation of whole layers in pixels. In this report the PES phenomenon could be healed by thermal treatment at temperatures below 100°C in the presence of oxygen. This indicates that the defects become just oxidized in the presence of minimal molecular (translational) movement by thermodynamic effects, which means that the fundamental defects such as voids in either among molecules or between layers cannot be completely recovered.

In this work we have attempted to cure these defects by melting organic layers, particularly focusing on a hole-injecting layer (HIL) that is the first layer contacting the anode of passive matrix (PM) OLED display (see the cross-sectional device structure in Fig. 1a). The process time of HIL melting was controlled as short as possible in order to

avoid a large scale deformation of the HIL layer geometry, whilst the melting process temperature chosen was above the intrinsic melting point of HIL material to make the melting effect in short time. The influence of HIL melting was examined with variations of pixel current together with monitoring the quality of displaying images in operation.

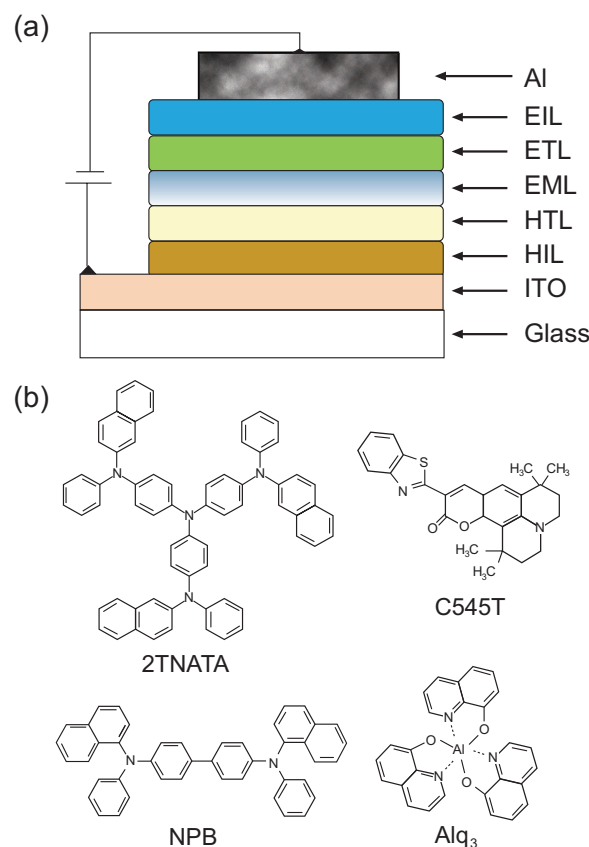


Fig. (1). (a) Cross-sectional device structure of PM-OLED display and (b) chemical structure of materials used for each layer (see the experimental section for full names of each layer and material).

*Address correspondence to this author at the Department of Chemical Engineering, Kyungpook National University, Sankuk-dong, Daegu 702-701, Republic of Korea; Tel: +82-53-950-5616; Fax: +82-53-950-5616; E-mail: ykimm@knu.ac.kr

Using a home-built photoengraving system equipped with spin-coater, spin-dryer, mask aligner and wet stations in clean room, indium-tin oxide (ITO) coated glass substrates (sheet resistance = $9 \Omega/\square$) were patterned to 128 lines of ITO stripes (width = 240 μm ; length = 41 mm). The patterned ITO-glass substrates were cleaned using acetone and isopropyl alcohol and then dried using a spin-dryer. On to these cleaned substrates, an inter-insulating layer (negative photoresist) was coated and processed to have an open area of 200 $\mu\text{m} \times 200 \mu\text{m}$ (note that the edges of ITO stripes were coated with the inter-insulating layer in order to avoid an electrical shortage owing to step coverage and/or spikes made upon etching process) [4]. After cleaning with UV-ozone (for 10 min), these substrates were put into a vacuum chamber to deposit a HIL.

The hole-injecting material used here is 4,4',4''-tris(*N*-(2-naphthyl)-*N*-phenylamino)-triphenylamine (2TNATA) (see Fig. 1b). The HIL (120 nm thick) was deposited at an evaporation rate of 0.1 nm/s in a vacuum of $\sim 3 \times 10^{-6}$ Torr. Some of these HIL coated substrates were put on a hot stage at 300 °C for 3 min to melt the coated HIL shortly. Next, a 20 nm thick hole-transporting layer (HTL), *N,N'*-di(naphthalen-1-yl)-*N,N'*-diphenylbenzidine (NPB), was deposited at 0.1 nm/s. Onto the HTL an emission layer (EML), which is a mix of tris(8-hydroxyquinolinato) aluminum (Alq_3) and 9-benzothiophenol-2-yl-1,1,6,6-tetramethyl-2,3,5,6,7a,11a-hexahydro-1H,4H-11-oxa-3a-aza-benzo[de]anthracen-10-one (C545T), was deposited as reported previously [8]. Then additional Alq_3 layer (20 nm thick) as an electron-transporting layer (ETL) was deposited on top of the EML, followed by depositing LiF (0.7 nm, 0.01 nm/s) as an electron-injecting layer (EIL) and Al cathode (120 nm, 0.5 nm/s) through a shadow mask (open width = 200 μm ; open length = 44 mm). The resulting OLED displays feature 128×128 pixels and 1.7 inch (diagonal) active image area. Finally these OLED displays fabricated were encapsulated with a conventional stainless steel canister attaching a desiccant film [4, 8].

Current-voltage (I-V) characteristics of OLED displays were measured using a specialized jig system, equipped with an electrometer (Keithley 238) and a multichannel scanner, which was designed to probe the current of each pixel. The average luminance of the present PM-OLED displays was measured using a candela meter (PR 650). Thermal transition behavior of 2TNATA was measured using a differential scanning calorimeter (DSC 2910, TA Instrument). The examination of active areas in each step was performed using an optical microscope (Olympus).

As illustrated schematically in Fig. (2), we assume that the defects in the HIL made upon thermal evaporation of 2TNATA are mainly voids and can be distributed in the bulk as well as in the surface of top and/or bottom of the HIL. If the HIL coated substrates are heated at a temperature above the melting point of 2TNATA, the void-like defects could be removed (cured) by the rearrangement of 2TNATA molecules (see Fig. 2b). So we need to know the exact thermal transition behavior of 2TNATA itself in order to decide the melting temperature of the HIL. As shown in Fig. (3), the first run DSC thermogram of 2TNATA powders shows glass transition at 120~145 °C, recrystallization at 175~223 °C, and melting at 235~275 °C (peak at 260 °C). After fully melting the sample, the glass transition range was slightly lower-

red to 110~125 °C (see the second run curve), whereas the peak temperature of recrystallization was shifted from 195 °C to 200 °C. These variations can be attributed to the closer packing of 2TNATA molecules after melting. However, we note that the melting point (~259 °C) in the second run was almost not changed after the first melting run.

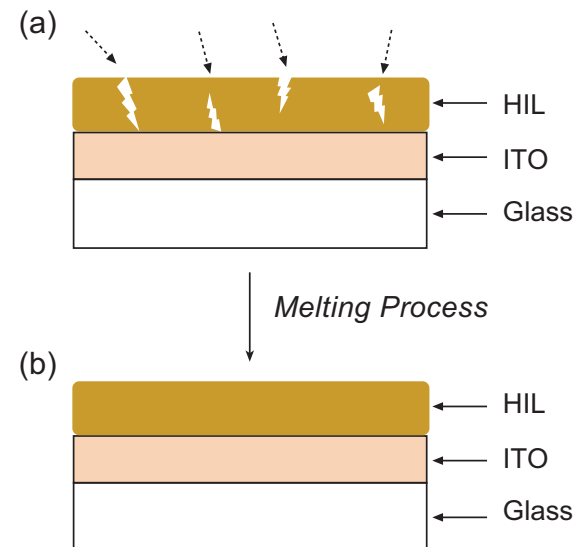


Fig. (2). Schematic illustration for curing void-like defects (indicated by arrows) in the untreated (as-coated) HIL (a) by melting the HIL, leading to defect-free HIL (b).

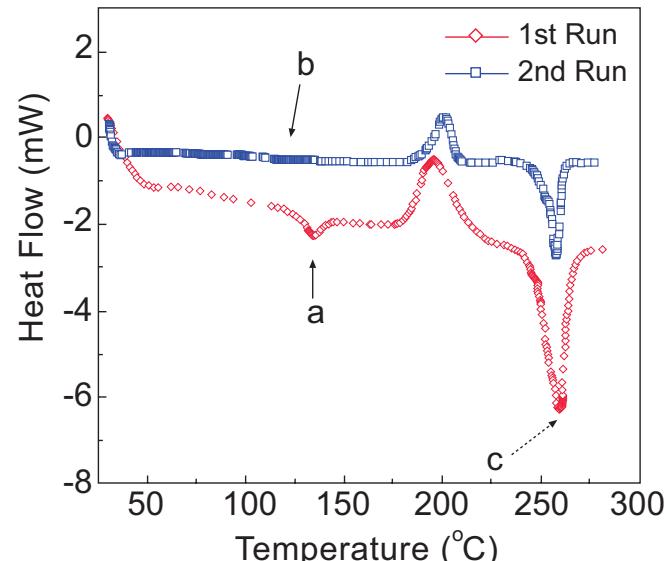


Fig. (3). DSC thermograms of 2TNATA that is used for the HIL in this work: 'a' and 'b' denote the glass transition ranges, whilst 'c' represents the melting point. The scan (heating) rate was 10 °C/min for both cases, whilst quenching of melts after the first run was performed automatically in the system by pouring liquid nitrogen stream.

Based on the DSC data, we chose 300 °C as the temperature for melting the HIL and then the heat treatment (melting) process was carried out for 3 min. Next, onto both substrates, subsequent layers were deposited as described in the experimental section to complete PM-OLED displays. Fig. (4) shows the single pixel J-V characteristics of the PM-OLED display with the untreated (as-coated) HIL. At for-

ward bias the major charge injection was initialized at around 3 V and the J-V curve shape was a diode type as usual (see Fig. 4a).

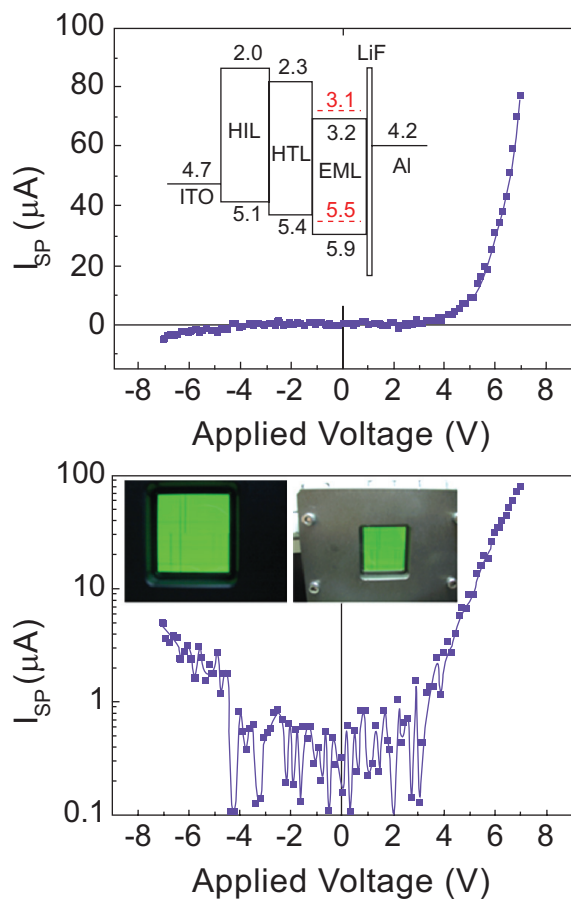


Fig. (4). (a) J-V curve of single pixel of the PM-OLED display with the untreated HIL (inset shows flat energy band diagram of this display) and (b) semilogarithmic J-V curve to highlight the reverse bias part (inset shows the photograph of displaying image in operation).

However, at reverse bias, the pixel current started to increase at around -3 V, which is obviously seen from the semilogarithmic J-V curve (see Fig. 4b). Considering the energy band structure (see inset to Fig. 4a) [9, 10], this reverse current is not expected at the low reverse bias (-3 V). Thus this reverse bias current can be assigned to the leakage current owing to a physical leakage path that is related to the presence of void-like defects claimed above. As a result, this PM-OLED display with the untreated HIL exhibited permanent black lines (in the displayed image) indicating cross-talks amongst anode and cathode electrodes after operating this display for about 1 hr (see inset image to Fig. 4b): We note that the time showing these black lines was quite varied sample by sample.

In contrast, the increasing reverse current was not measured for the PM-OLED display with the thermally treated (melted) HIL even though the reverse bias was extended to the voltage above -15 V (see Fig. 5a). This is also checked with the J-V curve in the semilogarithmic scale (see Fig. 5b). In addition, this display exhibited stable J-V characteristics

up to 15 V at forward bias. As a consequence, from this display with the thermally treated (melted) HIL, black (or even white) cross-talk lines were never observed during operation (duty cycle = 64, reverse off bias = -15 V, average brightness = 200 cd/m²) for more than 1000 hr (see inset image to Fig. 5b): we note that the display image test was carried out by fitting the PM-OLED display into a sample mobile phone case.

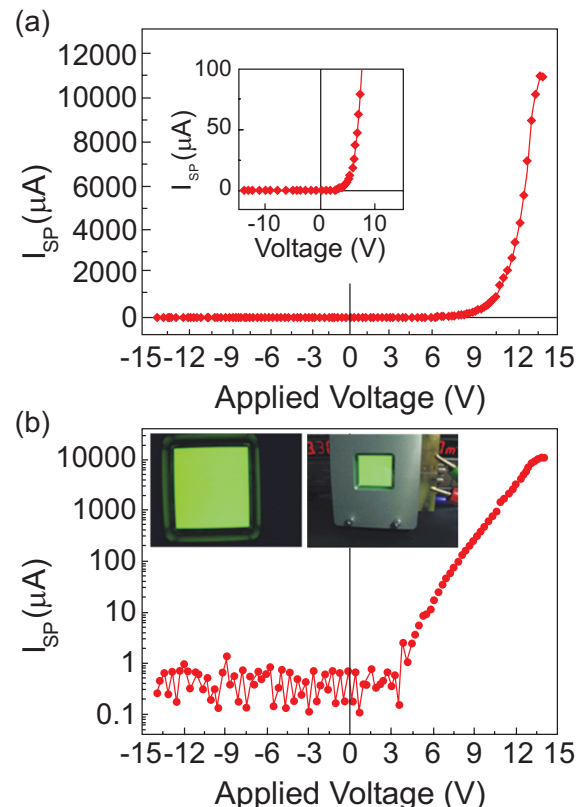


Fig. (5). (a) J-V curve of single pixel of the PM-OLED display with the thermally treated (melted) HIL (inset shows replotted J-V curve by reducing the y-axis scale to fit to the scale of Fig. 4a) and (b) semilogarithmic J-V curve to highlight the reverse bias part (inset shows the photograph of displaying image in operation).

In summary, we tried to melt the HIL coated on patterned substrates for making PM-OLED displays in order to cure void-like defects in the HIL. The HIL melting process was performed at 300 °C for 3 min. An increasing leakage current with voltage was measured at reverse bias for the display with the untreated HIL, whereas almost no leakage current was observed for the display with the thermally treated (melted) HIL. This result proves that void-like defects in the present HIL were cured (removed) by melting the HIL at this temperature shortly. The display images taken upon operation for long time also supported the superior reliability (stability) of the PM-OLED display with the thermally treated HIL. Hence we propose that the present HIL melting technology could greatly improve the reliability of PM-OLED displays and also we expect this could enhance the operational stability of OLED lighting.

ACKNOWLEDGEMENTS

The authors thank H. C. Ryu and S. H. Park for their help with display fabrication processes. This work was supported

by the Korea Science and Engineering Foundation (KOSEF) grant funded by the Korea government (No.R01-2007-000-10836-0).

REFERENCES

- [1] Tang, C. W.; VanSlyke, S. A. *Appl. Phys. Lett.*, **1987**, *51*, 913.
- [2] Burroughes, J. H.; Bradley, D. D. C.; Brown, A. R.; Marks, R. N.; Mackay, K. D.; Friend, R. H.; Burn, P. L.; Holmes, A. B. *Nature* (London), **1990**, *347*, 539.
- [3] Baldo, M. A.; O'Brien, D. F.; You, Y.; Shoustikov, A.; Silbey, S.; Thompson, M. E.; Forrest, S. R. *Nature* (London), **1998**, *395*, 151.
- [4] Kim Y.; Ha, C. S. *Advances in Organic Light-Emitting Device*; Trans Tech Publications: Switzerland/UK/USA, **2008**.
- [5] Hung, L. S.; Chen, C. H. *Mater. Sci. Eng. R.*, **2002**, *39*, 143.
- [6] Kwong, R. C.; Nugent, M. R.; Michalski, L.; Ngo, T.; Rajan, K.; Tung, Y.-J.; Weaver, M. S.; Zhou, T. X.; Hack, M.; Thompson, M. E.; Forrest, S. R.; Brown, J. J. *J. Appl. Phys. Lett.*, **2002**, *81*, 162.
- [7] Kim, Y.; Oh, E.; Choi, D.; Lim, H.; Ha, C. S. *Nanotechnology*, **2004**, *15*, 149.
- [8] Kim, Y.; Choi, D.; Lim, H.; Ha, C. S. *Appl. Phys. Lett.*, **2003**, *82*, 2200.
- [9] Kanno, H.; Hamada, Y.; Takahashi, H. *IEEE J. Sel. Top. Quant. Electron.*, **2004**, *10*, 30.
- [10] Haq, K.; Shan-peng, L.; Khan, M. A.; Jiang, X. Y.; Zhang, Z. L.; Zhu, W. Q. *Semiconduct. Sci. Technol.*, **2008**, *23*, 035024.

Received: March 31, 2008

Revised: June 27, 2008

Accepted: July 01, 2008

© Kim et al.; Licensee Bentham Open.

This is an open access article licensed under the terms of the Creative Commons Attribution Non-Commercial License (<http://creativecommons.org/licenses/by-nc/3.0/>) which permits unrestricted, non-commercial use, distribution and reproduction in any medium, provided the work is properly cited.